NASA TR R-115

NATIONAL AERONAUTICS AND SPACE ADMINISTRATION

TECHNICAL REPORT
R-115

METHOD FOR APPROXIMATING THE VACUUM MOTIONS OF SPINNING SYMMETRICAL BODIES WITH NONCONSTANT SPIN RATES

By C. WILLIAM MARTZ

1961

Case 1

TECHNICAL REPORT R-115

METHOD FOR APPROXIMATING THE VACUUM MOTIONS OF SPINNING SYMMETRICAL BODIES WITH NONCONSTANT SPIN RATES

By C. WILLIAM MARTZ

Langley Research Center
Langley Station, Hampton, Va.

TECHNICAL REPORT R–115

METHOD FOR APPROXIMATING THE VACUUM MOTIONS OF SPINNING SYMMETRICAL BODIES WITH NONCONSTANT SPIN RATES

By C. William Martz

SUMMARY

A method for approximating the vacuum motions of spinning rigid symmetrical bodies with varying spin rates and inertias has been completed. The analysis includes the effects of time varying thrust misalinements, mass unbalance, and jet damping. Results are given in the form of equations for space-referenced Euler angles, flight-path angles, body-referenced attitude rates, and earth-referenced vehicle-trajectory coordinates. The method consists of dividing the problem into intervals during which the time-dependent variables are assumed constant at their mean interval value. In order to check this procedure, solutions for various interval sizes are compared with solutions obtained with numerical methods. Although the method is somewhat lengthy for accurate hand computation in most cases, it is readily programed for machine solutions. Probably more important, the general solutions give insight into the separate effects of the variables and, in many cases, can be quickly used to determine the approximate ranges of the variables required for the desired solution to a given problem. In this respect, equations for determining maximum wobble have been derived for certain input conditions.

The method has been shown to compare closely with the numerical solutions of two sample problems. The sample problems also illustrated the relatively large effect of pitch and yaw jet damping on body motions.

INTRODUCTION

Vacuum motions of rotating bodies are becoming more important with the fairly recent ability to place objects in motion beyond the atmosphere. Machine computer programs for calculating these type motions have been completed and used successfully for some time. However, not everyone has a computer machine available for this work. Also, those with machines are using the trial-and-error process in most instances when locating the proper range of variables with the result that much machine time could be saved if some insight were available as to the individual effects of the different variables on the motions. This insight is best provided by analytical solutions to the equations of motions. There have been many papers published concerning this problem. (See, for example, refs. 1, 2, and 3.) However, one thing common to these papers has been the constant spin rate requirement. Other requirements sometimes include constant mass and inertia parameters or constant moment inputs. Solutions are sometimes limited to angular rates referred to a body-axis system requiring transformation and numerical integration to obtain space-referenced attitude angles.

The present paper presents an approximation method for determining the vacuum motion of spinning symmetrical rigid bodies with changing spin rates and inertias including the effects of time varying thrust misalinement, mass unbalance, and jet damping. Results are presented in the form of equations for space-referenced Euler angles and flight-path angles, and earth-referenced vehicle-trajectory coordinates. An expression for body-referenced attitude rates is included for convenience. The method consists of dividing the problem into intervals during which the time-dependent variables are assumed constant at their mean interval value. In order to check this procedure, solutions for various interval sizes are compared with solutions obtained with numerical methods. The method was developed under the

limitations that body pitch and yaw attitudes are restricted to "small angle" oscillations and that body moments of inertia about the pitch and yaw axes are equal.

SYMBOLS

a arbitrary fitting constant

A, B, C complex input coefficients defined in equation (13)

A_n, B_n fitting constants for moment inputs

A_4, A_5 constants defined by equations (18)

B_4, B_5, B_6, B_7 constants defined by equations (18)

C_1, C_2, C_3, C_4 constants defined by equations (18)

F magnitude of total asymmetrical force on vehicle

F_n, G_n input coefficients defined in equation (13)

$\overline{F}$ mean value of $F/(mV)$ within an interval

g constant of gravitational acceleration

I_X, I_Y, I_Z moments of inertia about X-, Y-, and Z-axes, respectively

I_{XY}, I_{XZ} products of inertia due to unbalance

$I=I_Y=I_Z$

$i=\sqrt{-1}$

j jet damping coefficient, K/I

$\overline{j}$ mean value of j over the interval

K pitch and yaw jet damping factor, $\dot{I}-\dot{m}l^2$

K' roll jet damping factor

l distance from body center of gravity to motor nozzle exit measured along X-axis

m mass of body

M_X, M_Y, M_Z asymmetrical moments about X-, Y-, and Z-axes, respectively

p, q, r angular velocity about X-, Y-, and Z-axes, respectively

$\overline{p}$ mean value of p within an interval

$\mathbf{R}_1, \mathbf{R}_2, \mathbf{R}_3$ vectors defined in equations (9)

T thrust

$\overline{T}$ mean value of $T/(mV)$ within the interval

t time from beginning of interval

V velocity of body along flight path

X, Y, Z orthogonal body-axis system (origin at body center of gravity)

x, y, z orthogonal space-axis system (origin arbitrary)

x_e, y_e, z_e x-, y-, and z-axis system rotated about y-axis to make z_e-axis vertical

α body angle of attack referred to a rolling body-axis system

α_s body angle of attack referred to a nonrolling body-axis system

β body angle of sideslip referred to a rolling body-axis system

β_s body angle of sideslip referred to a nonrolling body-axis system

$\overline{\beta}=\overline{j}+i(\overline{p}-\overline{\omega})$

γ_o' angle between x-, y-, and z-axis system and x_e, y_e, and z_e system in xz-plane

$\gamma=\gamma_\theta+i\gamma_\psi$

γ_θ flight-path angle in pitch plane

γ_ψ flight-path angle in yaw plane

λ vehicle total yaw angle, $\theta+i\psi$, radians

η_Y, η_Z angle between body principal X-axis and X (body reference) axis measured about Y- and Z-axes, respectively (see figs. 3 and 4)

$\phi_o=\int p dt$ at t_o

ψ, θ, ϕ yaw, pitch, and roll orientation angles of body X-, Y-, and Z-axes with respect to x, y, and z space-axis system (Euler angles)

ϕ' angle between the total asymmetrical force vector (always in the YZ-plane) and the $-Z$ direction (see fig. 1(b))

$\overline{\omega}$ mean value of pI_X/I within the interval

Subscripts:

o value of quantity at beginning of interval

f value of quantity at end of interval

max maximum value of quantity

n integer 1, 2, 3

A dot over a symbol indicates the first derivative with respect to time; a double dot indicates the second derivative with respect to time.

ANALYSIS

The modified Eulerian dynamic equations governing the rotational motions of a body about its

principal axes are (see refs. 4 and 5):

$$M_X = I_X\dot{p} - rq(I_Y - I_Z) + K'p \tag{1}$$

$$M_Y = I_Y\dot{q} - rp(I_Z - I_X) + Kq \tag{2}$$

$$M_Z = I_Z\dot{r} - pq(I_X - I_Y) + Kr \tag{3}$$

Figure 1 illustrates the axis system used.

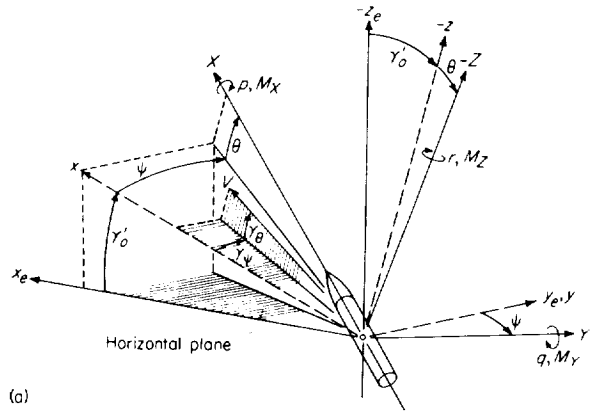

(a) Pitch and yaw orientation of axes systems. $\phi = 0$.

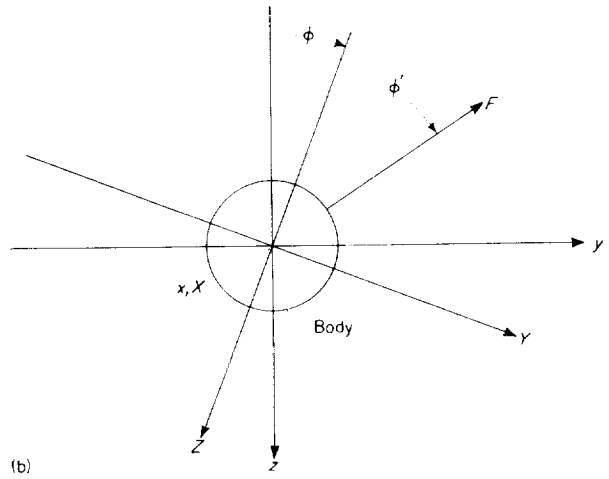

(b) Roll orientation of axes systems. $\theta = \psi = 0$.

FIGURE 1.—Axes systems employed in analysis.

If the body is assumed to have rotational mass symmetry, I_Z will be equal to I_Y and the rolling motion will not be affected by the pitching and yawing motions. This allows equations (2) and (3) to be solved independently of (1) for preselected p histories.

By multiplying equation (3) by i and adding the result to equation (2) with the rotational symmetry assumption, the equation becomes

$$M_Y + iM_Z = I(\dot{q} + i\dot{r}) + ip(I - I_X)(q + ir) + K(q + ir) \tag{4}$$

This equation can be referred from a rolling body-axis system to a space-axis system with the transformation equations (ref. 6)

$$\left.\begin{aligned} \dot{\theta} &= q\cos\phi - r\sin\phi \\ \dot{\psi} &= \left(\frac{1}{\cos\theta}\right)(q\sin\phi + r\cos\phi) \\ \dot{\phi} &= p + \dot{\psi}\sin\theta \end{aligned}\right\} \tag{5}$$

Now, for small values of θ when $\cos\theta \approx 1$ and $\dot{\psi}\sin\theta \ll p$ (zero reference for θ can be changed when necessary), equations (5) result in

$$\dot{\lambda} = \dot{\theta} + i\dot{\psi} = (q + ir)e^{i\phi} \tag{6}$$

where

$$\phi = \int_0^t p\,dt + \phi_o$$

Combining equations (4) and (6) yields

$$\ddot{\lambda} + \dot{\lambda}\left(j - ip\frac{I_X}{I}\right) = \left(\frac{M_Y + iM_Z}{I}\right)e^{i\left(\int_0^t p\,dt + \phi_o\right)} \tag{7}$$

where

$$j = \frac{K}{I} = \frac{\dot{I} - \dot{m}l^2}{I}$$

Equation (7) then governs the pitching and yawing motions of rotationally symmetric bodies referred to a space-axis system. The general form of solution for this equation is

$$\lambda = \theta + i\psi$$

$$= e^{i\phi_o}\int_0^t \left[e^{-\int_0^t \left(j - ip\frac{I_X}{I}\right)dt}\right]\left[\int_0^t \left(\frac{M_Y + iM_Z}{I}\left\{e^{\int_0^t \left[j + ip\left(1 - \frac{I_X}{I}\right)\right]dt}\right\}\right)dt + \dot{\lambda}_o e^{-i\phi_o}\right]dt + \lambda_o \tag{8}$$

The problem now is to find time functions for the variables $\left(j, p, \frac{I_X}{I}, \frac{M_Y+iM_Z}{I}\right)$ which not only permit equation (8) to be evaluated but which also adequately approximate the time histories of these variables as they would exist in any practical problem.

SPECIFIC SOLUTIONS

Solution with variables constant.—The solution of equation (7) when $j, p, \frac{I_X}{I}, \frac{M_Y}{I}$, and $\frac{M_Z}{I}$ are constants is

$$\lambda=\theta+i\psi$$
$$=\mathbf{R}_1+\mathbf{R}_2e^{ip\left(\frac{I_X}{I}\right)t}+\mathbf{R}_3e^{ipt} \tag{9}$$

where

$$\mathbf{R}_1=\lambda_o-\frac{\dot{\lambda}_o}{\frac{ipI_X}{I}-j}+\frac{(M_Y+iM_Z)e^{i\phi_o}}{p^2(I-I_X)-iIpj}\left(1-\frac{1}{\frac{I_X}{I}-\frac{j}{ip}}\right) \tag{9a}$$

$$\mathbf{R}_2=\frac{\dot{\lambda}_oe^{-jt}}{\frac{ipI_X}{I}-j}+\frac{(M_Y+iM_Z)e^{i\phi_o-jt}}{p^2(I-I_X)-iIpj}\left(\frac{1}{\frac{I_X}{I}-\frac{j}{ip}}\right) \tag{9b}$$

$$\mathbf{R}_3=\frac{-(M_Y+iM_Z)e^{i\phi_o}}{p^2(I-I_X)-iIpj} \tag{9c}$$

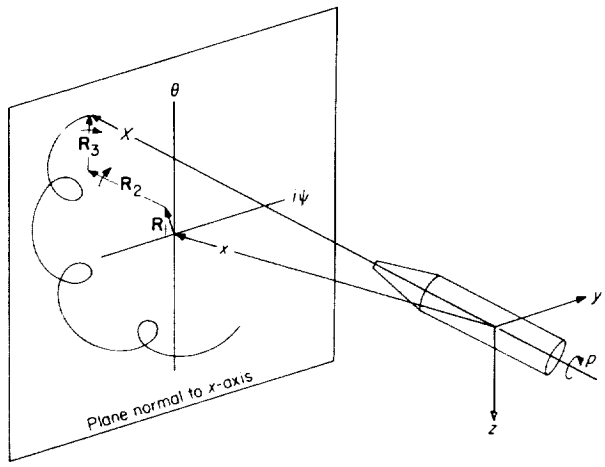

FIGURE 2.—Tricyclic motion (after ref. 1).

This λ solution can be thought of as the sum of three vectors: a nonrotating trim vector $\mathbf{R}_1$, a vector $\mathbf{R}_2$ rotating at the rate $\frac{pI_X}{I}$, and a vector $\mathbf{R}_3$ rotating at the rate p. This type of motion is referred to as "tricyclic" in reference 1 and illustrated in figure 2. The low-frequency vector is called the precession vector, and the high-frequency vector is called the nutation vector. Note that jet damping attenuates only the $\mathbf{R}_2$ vector. Equation (9) may be more familiar with $j=0$ and with the real parts separated from the imaginary parts as follows:

$$\theta=\theta_o+\frac{\dot{\theta}_o}{p\frac{I_X}{I}}\sin p\frac{I_Xt}{I}+\frac{\dot{\psi}_o}{p\frac{I_X}{I}}\left(\cos p\frac{I_Xt}{I}-1\right)+\frac{M_Y\cos\phi_o-M_Z\sin\phi_o}{p^2(I-I_X)}\left[1-\cos pt\right.$$
$$\left.+\frac{I}{I_X}\left(\cos p\frac{I_Xt}{I}-1\right)\right]-\frac{M_Z\cos\phi_o+M_Y\sin\phi_o}{p^2(I-I_X)}\left[-\sin pt+\frac{I}{I_X}\left(\sin p\frac{tI_X}{I}\right)\right] \tag{10a}$$

$$\psi=\psi_o-\frac{\dot{\theta}_o}{p\frac{I_X}{I}}\left(\cos p\frac{I_Xt}{I}-1\right)+\frac{\dot{\psi}_o}{p\frac{I_X}{I}}\sin p\frac{I_Xt}{I}+\frac{M_Y\cos\phi_o-M_Z\sin\phi_o}{p^2(I-I_X)}\left[-\sin pt+\frac{I}{I_X}\right.$$
$$\left.\left(\sin p\frac{I_Xt}{I}\right)\right]+\frac{M_Z\cos\phi_o+M_Y\sin\phi_o}{p^2(I-I_X)}\left[1-\cos pt+\frac{I}{I_X}\left(\cos p\frac{I_Xt}{I}-1\right)\right] \tag{10b}$$

Exact solution with nonconstant spin rates.—Of the many attempts to satisfy equation (8) by substitution of various time functions for the variables, the one which permitted an exact solution

with nonconstant spin rates used the substitutions

$$\left.\begin{aligned} p&=\frac{p_o}{1+at}\\ j&=0\\ \frac{I_X}{I}&=\text{Constant}\end{aligned}\right\} \tag{11}$$

The assumed straight line dependence of $1/p$ is quite practical especially if the problem is divided into time intervals. Although the constant-inertia-ratio requirement can be circumvented (by the method of the next section), the zero jet damping limitation is considered serious except, of course, for the case of nonthrusting vehicles.

Because a more general solution (presented in the next section) was found for equation (8) and in order to reduce confusion, the exact solution referred to in the present section is presented in appendix A along with all further discussion of this solution.

Mean value solution. - In the application of this solution, the problem is first divided into time intervals. The number and duration of these intervals depends upon the accuracy desired and will be discussed in the section entitled "Results and Discussion." Within each of the time intervals, the variables p, pI_X/I, and j are approximated by their mean value over that interval.

For example, consider the damping term in the exponentials of equation (8), namely, $\int_0^t j\,dt$. This integral is approximated by $\bar{j}t$ where $\bar{j}$ is the mean value of j over the interval. By definition, this is an exact approximation when the integration extends over the complete interval $\left(\text{i.e., } \int_0^{t_f} j\,dt \equiv \bar{j}t_f\right)$. For times less than one complete interval, however, the result is approximate. The accuracy of this approximation can be increased to any desired level by using shorter time intervals. Thus, with the substitutions

$$\left.\begin{aligned} p&=\bar{p}\\ p\frac{I_X}{I}&=\bar{\omega}\\ j&=\bar{j}\end{aligned}\right\} \tag{12}$$

a straightforward integration of the exponentials of equation (8) can be accomplished.

Concerning the moment inputs of equations (7) and (8), M_Y and M_Z should be approximated by functions which can adequately describe the variations of known time-dependent moment asymmetries such as thrust asymmetries, tip-off asymmetries, and dynamic unbalance effects. Remembering inertia must also be allowed to vary with time, the following input forms are assumed for each interval:

$$\frac{M_Y+iM_Z}{I}=\sum_{n=1}^{3}\left[(F_n+iG_n)(1+A_nt+B_nt^2)\right]=A+Bt+Ct^2 \tag{13}$$

When thrust or tip-off asymmetries are considered, M_Y and M_Z are the actual pitching- and yawing-moment asymmetries applied to the vehicle.

When dynamic unbalance effects are considered, the moments M_Y and M_Z are related to the pertinent variables as follows (ref. 4):

$$M_Y+iM_Z=I_{XZ}(r^2-p^2)+I_{XY}(\dot{p}+rq)+i[I_{XZ}(\dot{p}-qr)+I_{XY}(p^2-q^2)] \tag{14a}$$

which, for the present purposes, reduces to

$$M_Y+iM_Z=p^2(-I_{XZ}+iI_{XY})\approx p^2(I-I_X)(\eta_Y+i\eta_Z) \tag{14b}$$

since the products of inertia are related to angular deviations of the principal axes as follows:

$$\tan 2\eta_Y=\frac{2I_{XZ}}{I_X-I_Z}$$

and

$$\tan 2\eta_Z=\frac{2I_{XY}}{I_Y-I_X}$$

Now, if a combination of asymmetries and unbalance exist during the same interval, it may be easier to fit each asymmetry or unbalance to a separate complex input term. For example, the unbalance input $p^2\left(\frac{I_X}{I}-1\right)(\eta_Y+i\eta_Z)$ may be fitted to the term $(F_1+iG_1)(1+A_1t+B_1t^2)$. If the input moments have large or rapid changes in direction during an interval, however, it is more satisfactory to combine the real components of the various inputs separately from their imaginary components. Then, the total complex input is

fitted to a combination of two or more input terms as

$$(M_Y+iM_Z)_{total}=(F_1+0i)(1+A_1t+B_1t^2)+(0+iG_2)(1+A_2t+B_2t^2)$$

Now, when equations (8), (12), and (13) are combined, equation (8) becomes

$$\lambda=e^{i\phi_0}\int_0^t\left\{e^{(-\bar{j}+i\bar{\omega})t}\left[\int_0^t(A+Bt+Ct^2)e^{\bar{j}t+i(\bar{p}-\bar{\omega})t}dt+\dot{\lambda}_0e^{-i\phi_0}\right]\right\}dt+\lambda_0 \quad (15)$$

By integration,

$$\dot{\lambda}=\left[\dot{\lambda}_0-\frac{e^{i\phi_0}}{\bar{\beta}}\left(A-\frac{B}{\bar{\beta}}+\frac{2C}{\bar{\beta}^2}\right)\right]e^{(i\bar{\omega}-\bar{j})t}+\frac{e^{i(\bar{p}t+\phi_0)}}{\bar{\beta}}\left[\left(A-\frac{B}{\bar{\beta}}+\frac{2C}{\bar{\beta}^2}\right)+t\left(B-\frac{2C}{\bar{\beta}}\right)+t^2C\right] \quad (16a)$$

and

$$\lambda=\lambda_0+e^{i\phi_0}\left\{\left[\dot{\lambda}_0e^{-i\phi_0}-\frac{1}{\bar{\beta}}\left(A-\frac{B}{\bar{\beta}}+\frac{2C}{\bar{\beta}^2}\right)\right]\frac{e^{(i\bar{\omega}-\bar{j})t}-1}{i\bar{\omega}-\bar{j}}+\frac{e^{i\bar{p}t}-1}{i\bar{p}\bar{\beta}}\left[A-\frac{2C}{\bar{p}^2}+\left(\frac{i}{\bar{p}}-\frac{1}{\bar{\beta}}\right)\left(B-\frac{2C}{\bar{\beta}}\right)\right]+\frac{e^{i\bar{p}t}}{i\bar{p}\bar{\beta}}\left[t^2C+t\left(B-\frac{2C}{\bar{\beta}}+\frac{2iC}{\bar{p}}\right)\right]\right\} \quad (16b)$$

where

$$\bar{\beta}=\bar{j}+i(\bar{p}-\bar{\omega})$$

Equations (16) predict the approximate rotational motions (space referenced) of spinning symmetrical bodies with changing spin rates and inertias including the effects of time varying thrust misalinements, mass unbalance, and jet damping. As in equation (9), the λ solution is tricyclic with a nonrotating trim vector, a vector rotating at the rate $\bar{\omega}$, and a vector rotating at the mean spin rate $\bar{p}$. By separating the real and imaginary parts of equation (16b), the solution may be more readily evaluated in the following form:

$$\theta=\frac{(-C_1\bar{j}+C_2\bar{\omega})(e^{-\bar{j}t}\cos\bar{\omega}t-1)}{\bar{\omega}^2+\bar{j}^2}+\frac{(C_1\bar{\omega}+C_2\bar{j})(e^{-\bar{j}t}\sin\bar{\omega}t)}{\bar{\omega}^2+\bar{j}^2}+(\theta_0-C_3)\cos\bar{p}t-(\psi_0-C_4)\sin\bar{p}t+C_3+\sum_{n=1}^{3}\left\{[A_4\cos(\bar{p}t+\phi_0)+A_5\sin(\bar{p}t+\phi_0)]\left[A_nt+B_nt^2-\frac{2B_n\bar{j}t}{\bar{j}^2+(\bar{p}-\bar{\omega})^2}\right]-[A_4\sin(\bar{p}t+\phi_0)-A_5\cos(\bar{p}t+\phi_0)]\left[\frac{2B_n(\bar{p}-\bar{\omega})t}{\bar{j}^2+(\bar{p}-\bar{\omega})^2}+\frac{2B_nt}{\bar{p}}\right]\right\} \quad (17a)$$

$$\psi=\frac{(-C_1\bar{j}+C_2\bar{\omega})(e^{-\bar{j}t}\sin\bar{\omega}t)}{\bar{\omega}^2+\bar{j}^2}-\frac{(C_1\bar{\omega}+C_2\bar{j})(e^{-\bar{j}t}\cos\bar{\omega}t-1)}{\bar{\omega}^2+\bar{j}^2}+(\theta_0-C_3)\sin\bar{p}t+(\psi_0-C_4)\cos\bar{p}t+C_4+\sum_{n=1}^{3}\left\{[A_4\cos(\bar{p}t+\phi_0)+A_5\sin(\bar{p}t+\phi_0)]\left[\frac{2B_n(\bar{p}-\bar{\omega})t}{\bar{j}^2+(\bar{p}-\bar{\omega})^2}+\frac{2B_nt}{\bar{p}}\right]+[A_4\sin(\bar{p}t+\phi_0)-A_5\cos(\bar{p}t+\phi_0)]\left[A_nt+B_nt^2-\frac{2B_n\bar{j}t}{\bar{j}^2+(\bar{p}-\bar{\omega})^2}\right]\right\} \quad (17b)$$

where

$$A_4=\frac{-F_n(\bar{p}-\bar{\omega})+G_n\bar{j}}{\bar{p}[\bar{j}^2+(\bar{p}-\bar{\omega})^2]} \quad (18a)$$

$$A_5=\frac{F_n\bar{j}+G_n(\bar{p}-\bar{\omega})}{\bar{p}[\bar{j}^2+(\bar{p}-\bar{\omega})^2]} \quad (18b)$$

$$C_1=\dot{\theta}_0+\sum_{n=1}^{3}(-B_4B_6+B_5B_7) \quad (18c)$$

$$C_2=\dot{\psi}_o+\sum_{n=1}^{3}(-B_5B_6-B_4B_7) \tag{18d}$$

$$C_3=\theta_o+\sum_{n=1}^{3}\left\{-\frac{B_7}{\bar{p}}\left[B_4-\frac{2B_n}{\bar{p}^2}-\frac{2(\bar{p}-\bar{\omega})B_n}{\bar{p}\bar{j}^2+\bar{p}(\bar{p}-\bar{\omega})^2}\right]-\frac{B_6}{\bar{p}}\left[B_5+\frac{A_n}{\bar{p}}-\frac{2B_n\bar{j}}{\bar{p}\bar{j}^2+\bar{p}(\bar{p}-\bar{\omega})^2}\right]\right\} \tag{18e}$$

$$C_4=\psi_o+\sum_{n=1}^{3}\left\{-\frac{B_7}{\bar{p}}\left[B_5+\frac{A_n}{\bar{p}}-\frac{2\bar{j}B_n}{\bar{p}\bar{j}^2+\bar{p}(\bar{p}-\bar{\omega})^2}\right]+\frac{B_6}{\bar{p}}\left[B_4-\frac{2B_n}{\bar{p}^2}-\frac{2B_n(\bar{p}-\bar{\omega})}{\bar{p}\bar{j}^2+\bar{p}(\bar{p}-\bar{\omega})^2}\right]\right\} \tag{18f}$$

$$B_4=1-\frac{A_n\bar{j}}{\bar{j}^2+(\bar{p}-\bar{\omega})^2}+\frac{2B_n[\bar{j}^2-(\bar{p}-\bar{\omega})^2]}{[\bar{j}^2-(\bar{p}-\bar{\omega})^2]^2+[2\bar{j}(\bar{p}-\bar{\omega})]^2} \tag{18g}$$

$$B_5=-\frac{A_n(p-\bar{\omega})}{\bar{j}^2+(\bar{p}-\bar{\omega})^2}-\frac{4\bar{j}B_n(\bar{p}-\bar{\omega})}{[\bar{j}^2-(\bar{p}-\bar{\omega})^2]^2+[2\bar{j}(\bar{p}-\bar{\omega})]^2} \tag{18h}$$

$$B_6=\bar{p}(A_5\cos\phi_o-A_4\sin\phi_o) \tag{18i}$$

$$B_7=\bar{p}(A_5\sin\phi_o+A_4\cos\phi_o) \tag{18j}$$

Because body motions referred to a body-axis system are sometimes desired, equations (16a) and (6) are combined to obtain for reference

$$q+ir=\left[(q_o+ir_o)-\frac{1}{\beta}\left(A-\frac{B}{\beta}+\frac{2C}{\beta^2}\right)\right]e^{[i(\bar{\omega}-\bar{p})-\bar{j}]t}+\frac{1}{\beta}\left[\left(A-\frac{B}{\beta}+\frac{2C}{\beta^2}\right)+t\left(B-\frac{2C}{\beta}\right)+t^2C\right] \tag{19a}$$

or

$$q+ir=(\dot{\theta}+i\dot{\psi})e^{-i(\bar{p}t+\phi_o)} \tag{19b}$$

FLIGHT-PATH ATTITUDE

Up to this point, all effort has been toward determining the attitude of the body expressed by the Euler angles θ and ψ. Of greater importance to many investigations is the knowledge of how the external forces and moments on the body affect its velocity vector and space location. The author's interest in an analytical solution to this phase of the general problem was stimulated by the analytical results of reference 3. The method of reference 3 will now be used to extend the attitude solution of the present paper to expressions defining the velocity vector.

The force equation normal to the flight path in the pitch plane (fig. 3) is

$$mV\dot{\gamma}_\theta=-T\sin\alpha_s-mg\cos(\gamma_\theta+\gamma_o')+F\cos\alpha_s\cos\left(\int_0^t p\,dt+\phi_o+\phi'\right) \tag{20a}$$

and in the yaw plane (fig. 4) is

$$mV\dot{\gamma}_\psi=-T\sin\beta_s+F\cos\beta_s\sin\left(\int_0^t p\,dt+\phi_o+\phi'\right) \tag{20b}$$

By restricting the results to angular changes in velocity vector due to external disturbances other than gravity, the weight term of equation (20a) can be dropped. Multiplying equation (20b) by i, adding the result to equation (20a), and considering only small angles yields the following:

$$(\dot{\gamma}_\theta+i\dot{\gamma}_\psi)+(\gamma_\theta+i\gamma_\psi)\frac{T}{mV}=-\frac{T}{mV}(\theta+i\psi)+\frac{F}{mV}e^{i\left(\int_0^t p\,dt+\phi_o+\phi'\right)} \tag{21}$$

where

$$\theta=\alpha_s+\gamma_\theta$$

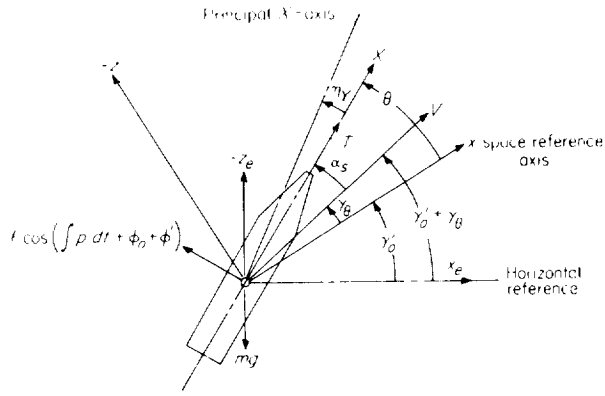

FIGURE 3. Pitch plane forces and angles. $\psi=\gamma_\psi=0$.

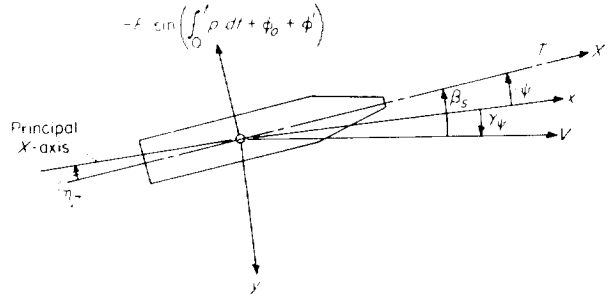

FIGURE 4. Yaw-plane forces and angles. $\theta=\gamma_\theta=0$.

and

$$\psi = -\beta_s + \gamma_\psi$$

The form of solution for equation (21) is

$$\gamma_\theta + i\gamma_\psi = e^{-\int_0^t \frac{T}{mV} dt} \left(\int_0^t \left\{ \frac{T}{mV} \left[\lambda + \frac{F}{T} e^{i\left(\int_0^t p dt + \phi_o + \varphi'\right)} \right] \left(e^{\int_0^t \frac{T}{mV} dt} \right) \right\} dt + \lambda_o \right) \tag{22}$$

Again, the mean value substitutions within the intervals are used. Let

$$\frac{T}{mV} = \overline{T} \tag{23}$$

$$\frac{F}{mV} = \overline{F} \tag{24}$$

Substituting equations (16), (23), and (24) into equation (22) and integrating gives

$$\begin{aligned} \gamma = \gamma_o e^{-\overline{T}t} + \frac{\overline{T} e^{i\phi_o}}{i\overline{p}\overline{\beta}(\overline{T} + i\overline{p})} \left\{ (e^{i\overline{p}t} - e^{-\overline{T}t}) \left[A - \frac{B}{\overline{\beta}} + \frac{2C'}{\overline{\beta}^2} + \frac{2C'}{(\overline{T} + i\overline{p})^2} + \left(B - \frac{2C'}{\overline{\beta}} + \frac{2iC'}{\overline{p}} \right) \left(\frac{i}{\overline{p}} - \frac{1}{\overline{T} + i\overline{p}} \right) \right] \right. \\ \left. + t \left(B - \frac{2C'}{\overline{\beta}} + \frac{2iC'}{\overline{p}} - \frac{2C'}{\overline{T} + i\overline{p}} \right) + t^2 C' \right\} + \left[\dot{\lambda}_o - \frac{e^{i\phi_o}}{\overline{\beta}} \left(A - \frac{B}{\overline{\beta}} + \frac{2C'}{\overline{\beta}^2} \right) \right] \left[\frac{e^{-\overline{T}t} - 1}{i\overline{\omega} - \overline{j}} + \frac{\overline{T}}{\overline{T} - \overline{j} + i\overline{\omega}} (e^{i\overline{\omega}t - \overline{j}t} - e^{-\overline{T}t}) \right] \\ + \frac{\overline{F} e^{i(\phi_o + \varphi')}}{\overline{T} + i\overline{p}} (e^{i\overline{p}t} - e^{-\overline{T}t}) + (1 - e^{-\overline{T}t}) \left\{ \lambda_o - \frac{e^{i\phi_o}}{i\overline{p}\overline{\beta}} \left[A - \frac{2C'}{\overline{p}^2} + \left(\frac{i}{\overline{p}} - \frac{1}{\overline{\beta}} \right) \left(B - \frac{2C'}{\overline{\beta}} \right) \right] \right\} \end{aligned} \tag{25}$$

Equation (25) predicts the direction of the velocity vector for vehicles having the angular motions described by equations (16). Note the similarity of these two solutions (eqs. (16b) and (25)). Both consist of a fixed vector, a vector rotating at the mean roll rate, and a vector rotating at the mean value of $\frac{pI_x}{I}$.

Again, it should be remembered that these solutions are for small values of θ and that flight-path curvature due to gravity is disregarded. An approximate change in flight-path angle due to gravity is

$$\Delta(\gamma_\theta + i\gamma_\psi) = -\frac{gt}{V_o} \cos \gamma_o' e^{-\overline{T}t}$$

The results of equations (16) and (25) can be combined to yield time histories of angle of attack and angle of sideslip as follows:

$$\left.\begin{aligned} \alpha_s &= \theta - \gamma_\theta \\ \beta_s &= -\psi + \gamma_\psi \end{aligned}\right\} \tag{26}$$

and because of the relationship

$$\beta + i\alpha = (\beta_s + i\alpha_s) e^{-i\phi}$$

$$\left.\begin{aligned} \alpha &= -\beta_s \sin(\overline{p}t + \phi_o) + \alpha_s \cos(\overline{p}t + \phi_o) \\ \beta &= \beta_s \cos(\overline{p}t + \phi_o) + \alpha_s \sin(\overline{p}t + \phi_o) \end{aligned}\right\} \tag{27}$$

Now, going on to the space-position solution, it can be shown from figure 1 that

$$\left.\begin{aligned} \dot{z}_e &= -V \sin(\gamma_\theta + \gamma_o') \\ \dot{x}_e &= V \cos(\gamma_\theta + \gamma_o') \cos \gamma_\psi \\ \dot{y}_e &= V \cos(\gamma_\theta + \gamma_o') \sin \gamma_\psi \end{aligned}\right\} \tag{28}$$

The force equation along the flight path for small disturbances is

$$T \cos \alpha \cos \beta - mg \sin(\gamma_\theta + \gamma_o') = m\dot{V} \tag{29}$$

By considering small angles for α and β and removing gravity effects equation (29) becomes

$$\frac{T}{mV} = \frac{\dot{V}}{V} \tag{30}$$

Integrating this equation and combining with equation (23) results in

$$V = V_o e^{\overline{T}t} \tag{31}$$

Now, this velocity expression can be substituted into equations (28) with the assumption that γ_θ and γ_ψ are small angles, and the equations can be expanded. Since equations (28) and (31) were obtained by neglecting the force of gravity, the term gt is added to the equation for $\dot{z}_e$ to get the earth-referenced velocity equations with gravity effects included.

$$\left.\begin{aligned} \dot{z}_e &= -V_o e^{\overline{T}t}(\gamma_\theta \cos \gamma'_o + \sin \gamma'_o) + gt \\ \dot{x}_e &= V_o e^{\overline{T}t}(\cos \gamma'_o - \gamma_\theta \sin \gamma'_o) \\ \dot{y}_e &= V_o e^{\overline{T}t}\gamma_\psi (\cos \gamma'_o - \gamma_\theta \sin \gamma'_o) \end{aligned}\right\} \tag{32}$$

Equations (32) are integrable and yield the space location equations with gravity effects included. The result is given here as functions of γ_θ and γ_ψ which are available from equation (25).

$$\left.\begin{aligned} z_e &= z_{e,o} - \frac{V_o \sin \gamma'_o}{\overline{T}}(e^{\overline{T}t} - 1) \\ &\quad - V_o \cos \gamma'_o \int \gamma_\theta e^{\overline{T}t} dt + \tfrac{1}{2} gt^2 \\ x_e &= x_{e,o} + \frac{V_o \cos \gamma'_o}{\overline{T}}(e^{\overline{T}t} - 1) \\ &\quad - V_o \sin \gamma'_o \int \gamma_\theta e^{\overline{T}t} dt \\ y_e &= y_{e,o} + V_o \cos \gamma'_o \int \gamma_\psi e^{\overline{T}t} dt \\ &\quad - V_o \sin \gamma'_o \int \gamma_\theta \gamma_\psi e^{\overline{T}t} dt \end{aligned}\right\} \tag{33}$$

RESULTS AND DISCUSSION

The results of this paper are primarily the attitude solutions expressed by equations (16), the flight-path direction expressed by equation (25), and the space-location solution of equations (33). All these solutions are complicated by the large number of variables which affect the end results. In order to show some of the more important interrelationships of these variables, others must be held constant.

ATTITUDE SOLUTION

With the attitude solution of equations (16), the separate motion effects of the initial attitude λ_o and the initial attitude rate $\dot{\lambda}_o$ can readily be demonstrated by making $A = B = C = 0$ and $\bar{j} = 0$ with the result that

$$\lambda = \lambda_o + \frac{\dot{\lambda}_o}{i\bar{\omega}}(e^{i\bar{\omega}t} - 1)$$

This solution is shown in figure 5(a) to be the sum of a fixed vector and a rotating vector. Until λ_o and $\dot{\lambda}_o$ are specified, however, it is not possible to say whether a higher or lower spin rate or inertia ratio will increase or decrease λ_{max}, the common performance standard of spin stabilization.

Now, if the model is thrusting but with no disturbance moments, jet damping normally attenuates the motion and the plot of θ against ψ turns into a logarithmic spiral as shown in figure 5(b).

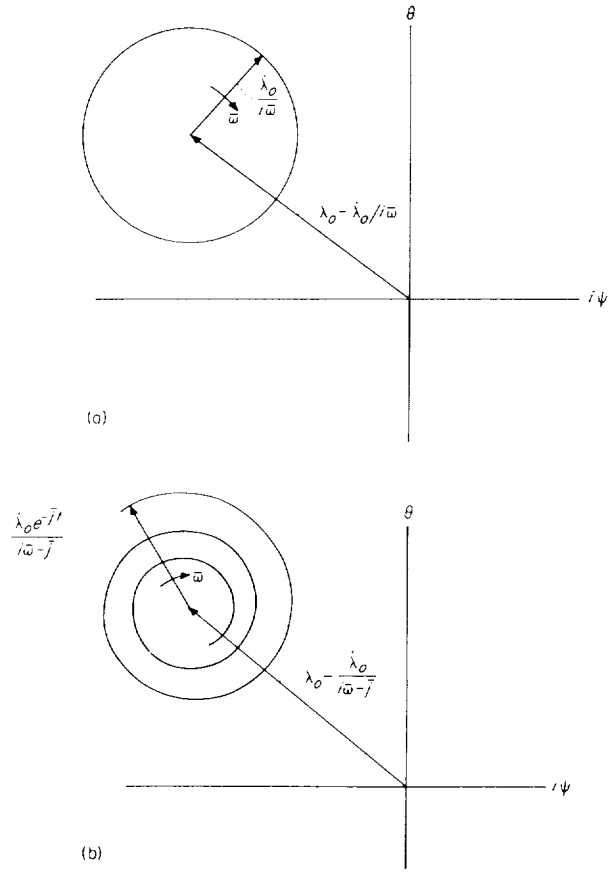

(a) $\bar{j} = 0$ (no jet damping).
(b) $\bar{j} > 0$ (with jet damping).

FIGURE 5. Sample attitude solution with no moment inputs ($F_n + iG_n = 0$).

Moment asymmetries. For the effects of moment asymmetries the solution for λ may be simplified by assuming no residual motion ($\lambda_o = \dot{\lambda}_o = 0$) and constant inputs ($B = C = 0$). Then for $\phi_o = 0$, the solution becomes

$$\lambda = \frac{M_Y + iM_Z}{iI\bar{p}[\bar{j} + i(\bar{p} - \bar{\omega})]}\left[e^{i\bar{p}t} - 1 + i\bar{p}\,\frac{1 - e^{(i\bar{\omega} - \bar{j})t}}{i\bar{\omega} - \bar{j}}\right]$$

Expressions for maximum wobble can be obtained from this equation under the following conditions: When $\omega < \bar{p}$, or, more accurately, when

$$\frac{\bar{p}}{\sqrt{\bar{\omega}^2 + \bar{j}^2}}\left[1 + e^{\frac{-\bar{j}\pi}{\bar{\omega}} + \frac{\bar{j}^2}{\bar{\omega}(\bar{p} - \bar{\omega})}}\right] > 2$$

then

$$\lambda_{max} = \sqrt{\frac{M_Y^2 + M_Z^2}{I^2}}\,\frac{1}{(\bar{\omega}^2 + \bar{j}^2)[\bar{j}^2 + (\bar{p} - \bar{\omega})^2]}\left[\sqrt{\left(1 - \frac{\bar{\omega}}{\bar{p}}\right)^2 + \left(\frac{\bar{j}}{\bar{p}}\right)^2} + \frac{\sqrt{\bar{\omega}^2 + \bar{j}^2}}{\bar{p}} + e^{\frac{-\bar{j}\pi}{\bar{\omega}} + \frac{\bar{j}^2}{\bar{\omega}(\bar{p} - \bar{\omega})}}\right]$$

at 1, for normally small j values (i.e., $\bar{j}/\bar{p} \ll 1$ and $\bar{j}/\omega \ll 1$),

$$\lambda_{max} \approx \frac{2\sqrt{M_Y^2 + M_Z^2}}{I\bar{\omega}(\bar{p} - \bar{\omega})}$$

When $\bar{\omega} > \bar{p}$, or, more precisely, when

$$\frac{\bar{p}}{\sqrt{\bar{\omega}^2 + \bar{j}^2}}\left[1 + e^{-(\bar{j}/\bar{p})\tan^{-1}(\bar{j}/\bar{\omega})}\right] < 2$$

then

$$\lambda_{max} = \sqrt{\frac{M_Y^2 + M_Z^2}{I}}\,\frac{1}{(\bar{\omega}^2 + \bar{j}^2)[\bar{j}^2 + (\bar{p} - \bar{\omega})^2]}\left[\sqrt{\left(\frac{\bar{\omega}}{\bar{p}} - 1\right)^2 + \left(\frac{\bar{j}}{\bar{p}}\right)^2} + \frac{\sqrt{\bar{\omega}^2 + \bar{j}^2}}{\bar{p}} + e^{-(\bar{j}/\bar{p})\tan^{-1}(\bar{j}/\bar{\omega})}\right]$$

and, for normally small j values,

$$\lambda_{max} \approx \frac{2\sqrt{M_Y^2 + M_Z^2}}{I\bar{p}(\bar{\omega} - \bar{p})}$$

Note that both λ_{max} expressions show that maximum wobble due to asymmetrical moments is proportional to the size of the moment and, for normally small $\bar{j}$ values, is effectively inversely proportional to the product of the mean roll inertia and the square of the mean spin rate over the interval. It follows, therefore, that spin-rate magnitudes increasing with time (as well as larger spin rates) will reduce wobble because of the resulting larger value of mean spin rate over the interval.

Lastly, for $\bar{p} \approx \bar{\omega}$, an expression for maximum wobble can be obtained under the reasonable conditions that $(\bar{j}/\bar{p}) \ll 1$ and that $(\bar{p} - \bar{\omega})t$ is a "small angle." This expression is

$$\lambda_{max} = \frac{1}{I\bar{p}}\sqrt{(M_Y^2 + M_Z^2)\,\frac{(1 - e^{-\bar{j}t})^2 + [e^{-\bar{j}t}(\bar{\omega} - \bar{p})t]^2}{\bar{j}^2 + (\bar{p} - \bar{\omega})^2}}$$

This solution indicates the divergent nature of λ_{max} for $\bar{p} \approx \bar{\omega}$ at small $\bar{j}t$ values. The divergence is more apparent for $\bar{j} = 0$ with the result

$$\lambda_{max} = \frac{t}{I\bar{p}}\sqrt{M_Y^2 + M_Z^2}$$

Although the quantity $(\bar{p} - \bar{\omega})$ is never exactly equal to zero in a practical problem, the theoretical possibility of $I = I_X$ also results in the simple divergence equation just given (for normally small values of $\bar{j}$). These divergence solutions reveal that wobble buildup is proportional to the input moment disturbances and to the time required for passing through the resonant condition $(\bar{p} \approx \bar{\omega})$ and inversely proportional to pitch or yaw inertia and mean spin rate.

Unbalance. It is difficult to show clearly the effects of unbalance on the motion of a body having a nonconstant spin rate because the input moments (eq. (14b)) are variable. Thus, the quantities B and C or A_n and B_n must take on values other than zero which precludes a simplified version of the general solution. However, by considering fixed p and $\frac{I_X}{I}$ values temporarily, equations (9) and (14b) can be combined (still retaining the conditions $\lambda_o = \dot{\lambda}_o = 0$, $B = C = 0$, and $\phi_o = 0$) with the result

$$\lambda = \frac{\eta_Y + i\eta_Z}{i\frac{jI}{p(I - I_X)} - 1}\left[e^{ip\frac{I_X}{I}t} - 1 + ip\,\frac{1 - e^{\left(ip\frac{I_X}{I} - j\right)t}}{ip\frac{I_X}{I} - j}\right]$$

When $\frac{I_X}{I} < 1$, $\lambda_{max} =$

$$\sqrt{\left[1+\left(\frac{Ij}{pI-pI_X}\right)^2\right]\left[\left(\frac{I_X}{I}\right)^2+\left(\frac{j}{p}\right)^2\right]}\left(1+e^{\frac{-j\pi I}{pI_X}}\right)\sqrt{\eta_Y{}^2+\eta_Z{}^2}$$

and, for normally small values of j,

$$\lambda_{max} \approx \frac{2I}{I_X}\sqrt{\eta_Y{}^2+\eta_Z{}^2}$$

When $\frac{I_X}{I} > 1$

$$\lambda_{max} = 2\sqrt{\frac{\eta_Y{}^2+\eta_Z{}^2}{1+\left[\frac{Ij}{p(I-I_X)}\right]^2}}$$

and, for normally small values of j,

$$\lambda_{max} \approx 2\sqrt{\eta_Y{}^2+\eta_Z{}^2}$$

When $\frac{I_X}{I}=1$,

$$\lambda_{max} = 0$$

These results are for constant values of p and $\frac{I_X}{I}$ with no residual motions. Note that wobble due to unbalance is independent of spin rate except through the jet damping terms which normally have only a very small effect. Thus, wobble due to unbalance cannot be controlled by spinning as can, for example, the wobble resulting from initial attitude rates or thrust misalinement.

APPLICATION

The analytical expressions for λ and γ given in the present paper have been programed for use with an IBM 7090 electronic data processing machine. Sample problems were composed and this program used to generate their solutions. The numerical solutions to these problems were also obtained with the numerical integration method reported in reference 3 for the purpose of comparison with approximate solutions.

It should be mentioned that the values for $\overline{p}$, $\overline{\omega}$, $\overline{T}$, and $\overline{F}$ used in the approximate solutions were based on assumed exponential histories of the variables within the interval (i.e., for example, $\overline{p} = \frac{p_f - p_o}{\log_e \frac{p_f}{p_o}}$). Although this assumption of exponential dependence of the variables is inherently more accurate, almost identical results (not shown) were obtained with the approximate method by assuming linear histories of the variables within each interval $\left(\text{i.e., } \overline{p} = \frac{p_f + p_o}{2}\right)$.

The first application was to simulate the motions of a rocket model which was the last stage of a multistage rocket system. The model can be thought of as a cylinder about 1¼ feet in diameter and 3¾ feet in length having a ratio of fuel weight to total weight of 1/2. An angular thrust asymmetry of 0.001 radian in both the pitch and yaw planes provided a continuous disturbance to the motion. A separate spin motor was assumed to increase model spin rate during the problem from 5 to 9 radians per second. The approximate solution was computed with two intervals and with ten intervals, each with and without jet damping. Problem constants and initial conditions are listed in appendix B. Results are shown in figures 6 to 8.

Figure 6(a) shows the approximate θ and ψ histories obtained with the two-interval solution (no jet damping) and their comparison with the numerical solution. In general, this comparison indicates a good approximation of the numerical solution except for the first negative peaks of each curve where the approximate solution underestimates the actual values. The phase difference between the approximate and numerical solutions is to be expected and is usually of little importance. In this respect, both ends of all intervals are exactly in phase, the greatest difference occurring halfway through each interval. The two-interval solution for flight-path direction is shown in figure 6(a) along with the numerical solution. Here, the comparison appears not quite so good as the attitude solution, but satisfactory for most purposes.

In order to illustrate the accuracy obtained with many intervals, the ten-interval solution of figure 6(b) was computed. Note the improvement in the λ and γ solutions as compared with the two-interval results.

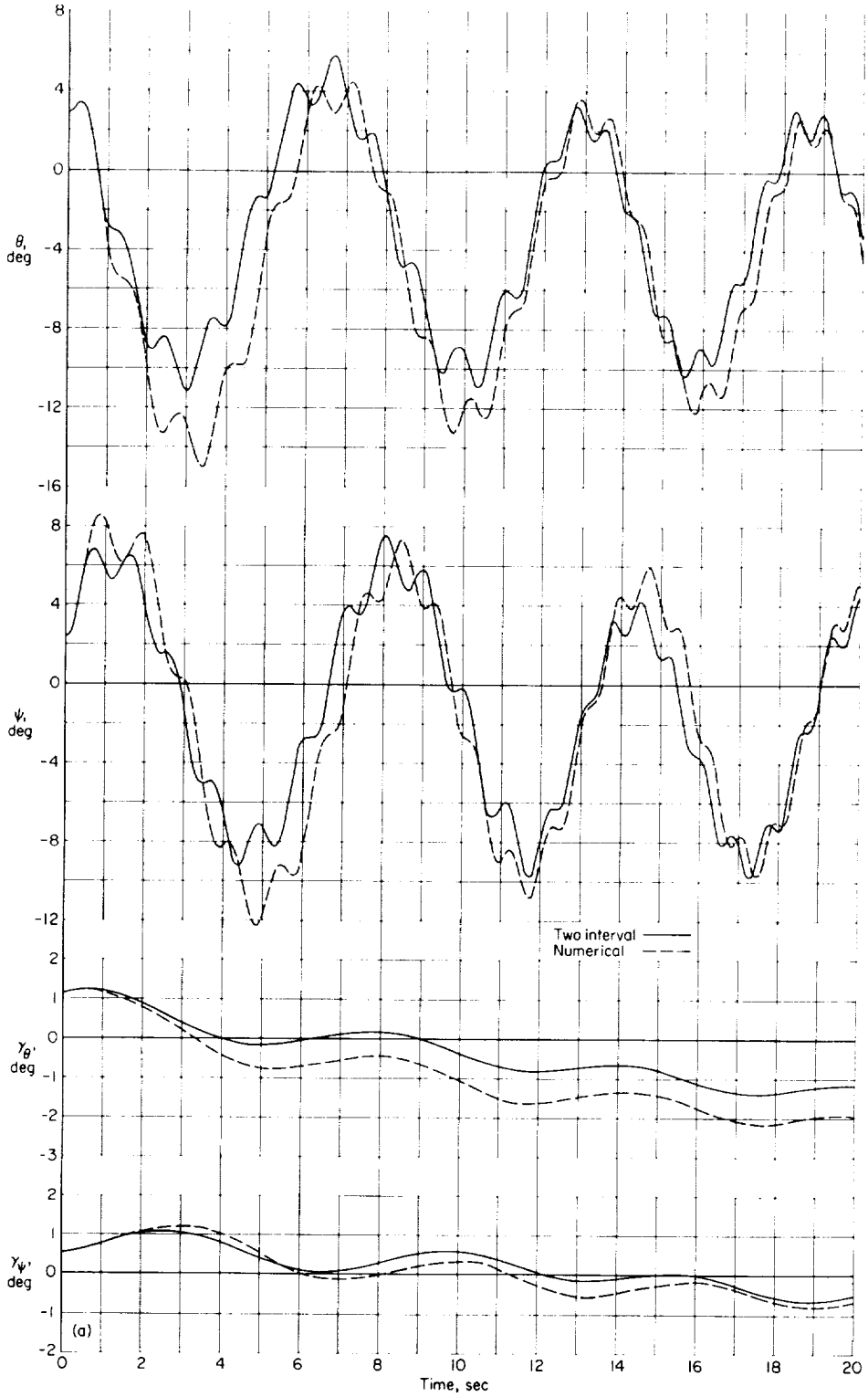

(a) Two-interval approximation.

FIGURE 6. Approximate and numerical solutions of first sample problem. $\bar{j}=0$.

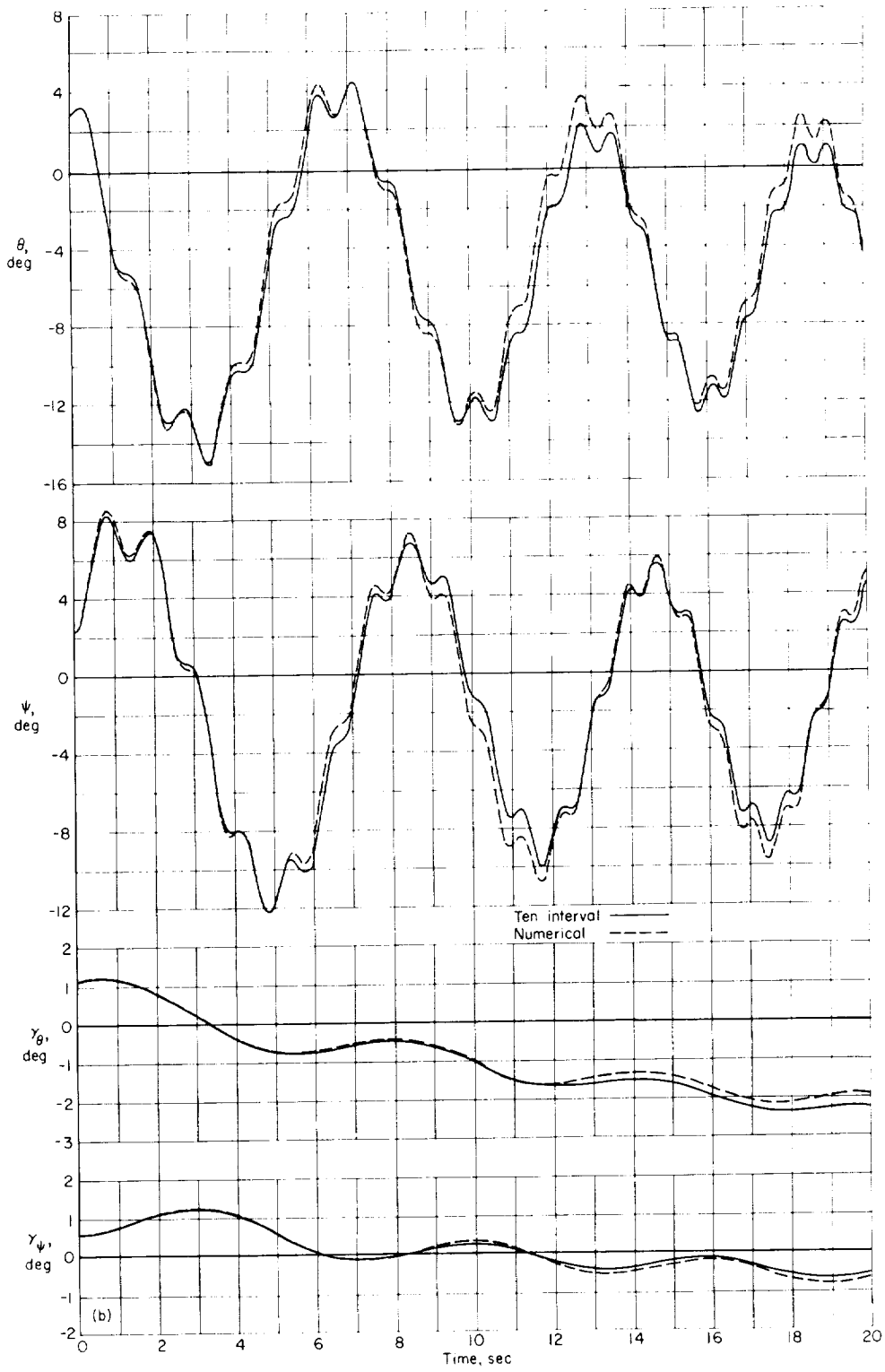

(b) Ten-interval approximation.

FIGURE 6. - Concluded.

Thus far, problem cases have been restricted to zero jet damping because the program used to obtain the numerical solutions does not include jet-damping effects. However, jet-damping effects can be quite large as illustrated in figure 7. This figure presents the ten-interval solution with and without jet damping. Note the large attenuation effect of jet damping on the low-frequency (precession) mode and the near absence of this effect on the high-frequency mode. This large damping effect is not unusual and can even be called typical. Its presence is fortunate since no other forces are naturally available to damp the motion.

It is well documented that bodies having $I_X = I_Y = I_Z$ cannot be spin stabilized. However, the motions of axisymmetric bodies passing through this condition are not well known. For this reason, the second type of problem for simulation was selected to reveal the effects of passing through inertial resonance $\left(\frac{I_X}{I}=1\right)$. This problem assumed a variable I_X, a constant I, and no roll inputs. Only the λ solution was computed for purposes of simplicity. The problem was computed with one interval, two intervals, and three intervals, in all cases with no jet damping. The necessary constants and initial conditions are presented in appendix B. Results are presented in figure 8 which also shows the numerical solution for comparison purposes. Figure 8 illustrates the one-interval solution of this problem to be inadequate. The two-interval solution is much improved and reveals the trends of the numerical solution. However, for an accurate amplitude comparison, the three-interval solution is indicated.

Intervals. Solutions have been previously described as one interval, two interval, and so forth, with no explanation of why or how the number of intervals was selected. As previously mentioned, a two-interval solution (for example) means that the problem is computed in two intervals, usually so as to result in about the same percentage changes of the variables within each interval. Then, closed solutions for the first interval are obtained with equations (16) and (25) along with the initial conditions of the problem. In order to compute the solutions at any time of the second interval, however, the final values of interval one must be calculated and used as initial conditions for the second interval.

While the number of computations increases with the number of intervals used, the accuracy of the results increases thereby. The optimum number of intervals, then, depends upon the computing facilities available, the degree of accuracy desired, and the total percentage change of variables throughout the problem. In this respect, the author has tentatively settled on using intervals in which the values of p or $p\frac{I_X}{I}$ do not vary more than about 15 percent for "accurate" results or more than about 30 percent for approximate results. These percentages are based on a limited amount of experience. Percentages for the sample problems are given in appendix B.

Computing time.—Computing times for sample problem number one of appendix B were obtained for both the approximate and the numerical or step-by-step solutions. These solutions were generated by an IBM 7090 electronic data processing machine and required certain compatibility changes since both programs were originally set up for the IBM 704 electronic data processing machine.

Both programs required about 26 seconds read-in time. Excluding read-in time, the approximate method (10-interval solution) had a ratio of machine time to problem time of about 0.93 and the numerical method a ratio of about 4.8. Reducing the number of intervals used in the approximate solution would decrease its ratio only a small amount.

Other factors involved in a computing time comparison are as follows: First, the numerical method is programed to yield output quantities not included in the output of the approximate method. It is estimated that the elimination of this part of the program would amount to about ⅓ reduction in computing time for the numerical method. Second, the above ratios are for defining the output every 0.1 second and could be reduced proportionally for the approximate method by using fewer output times. The numerical method would not benefit in this respect.

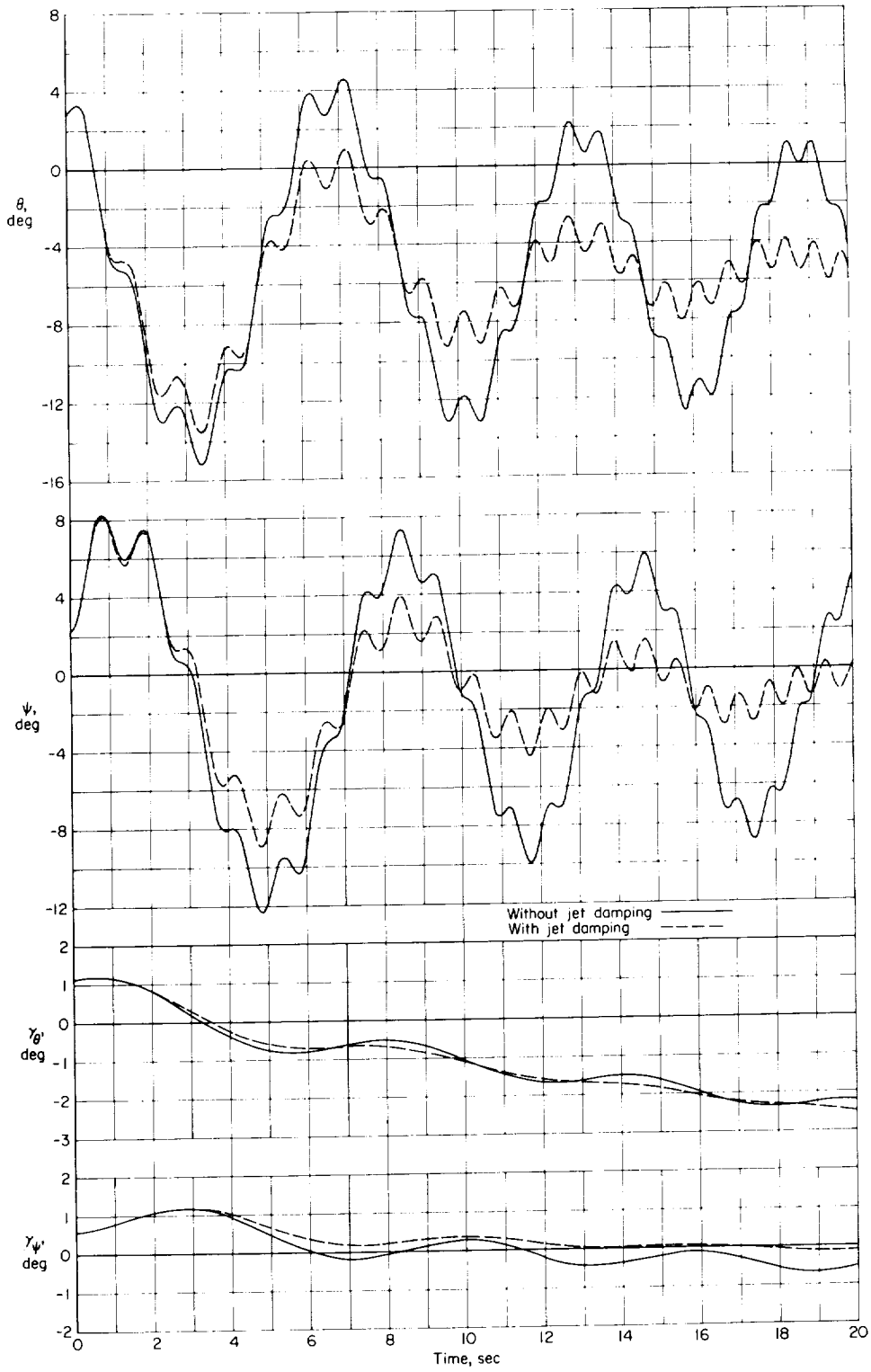

FIGURE 7. -Effects of jet damping in first sample problem. Ten-interval solutions.

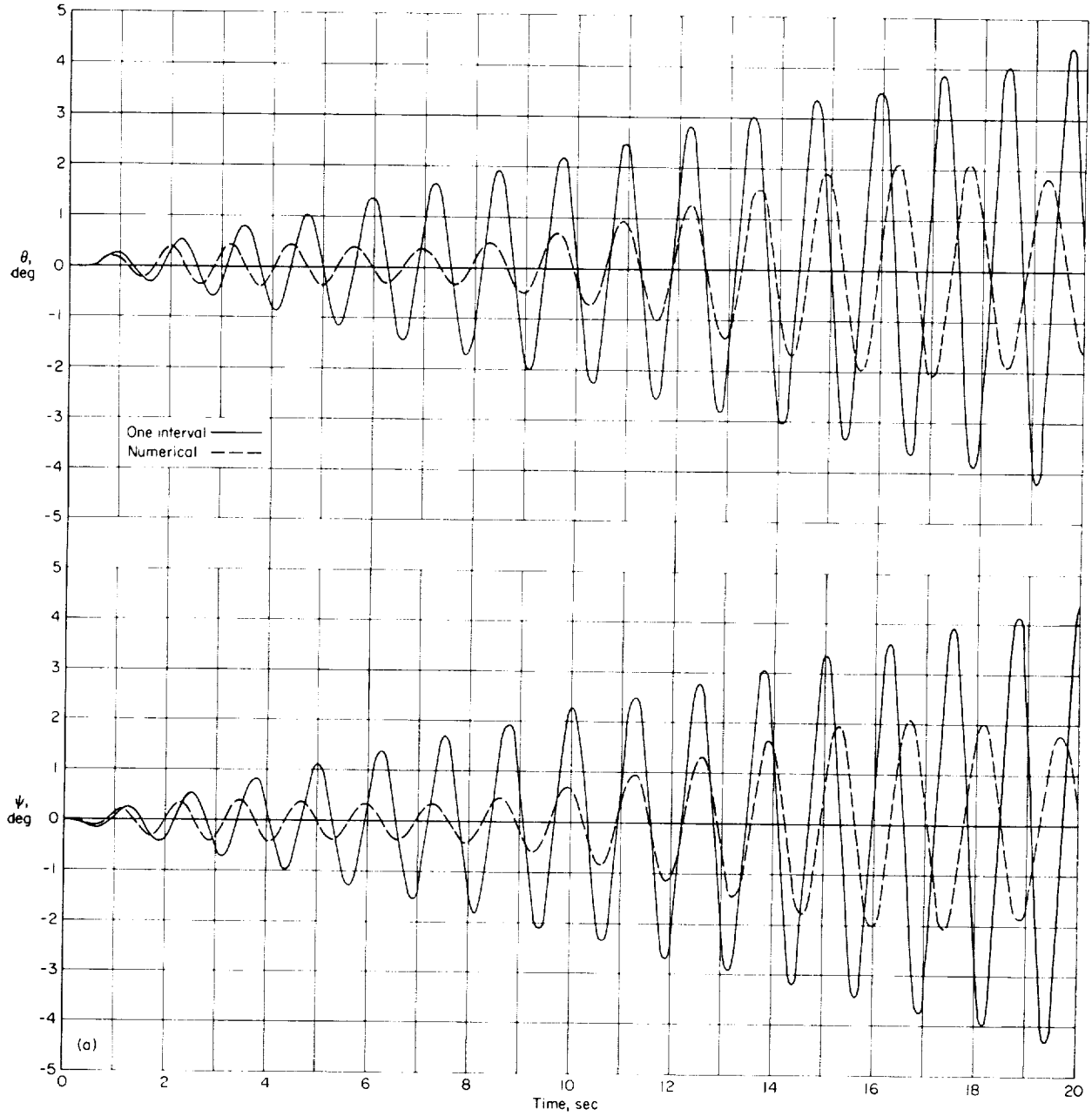

(a) One-interval approximation.

FIGURE 8.—Comparison of approximate and numerical solutions of second sample problem showing motions of a body passing through inertial resonance $\left(\frac{I_x}{I}=1\right)$ at $t=10$. $\bar{j}=0$.

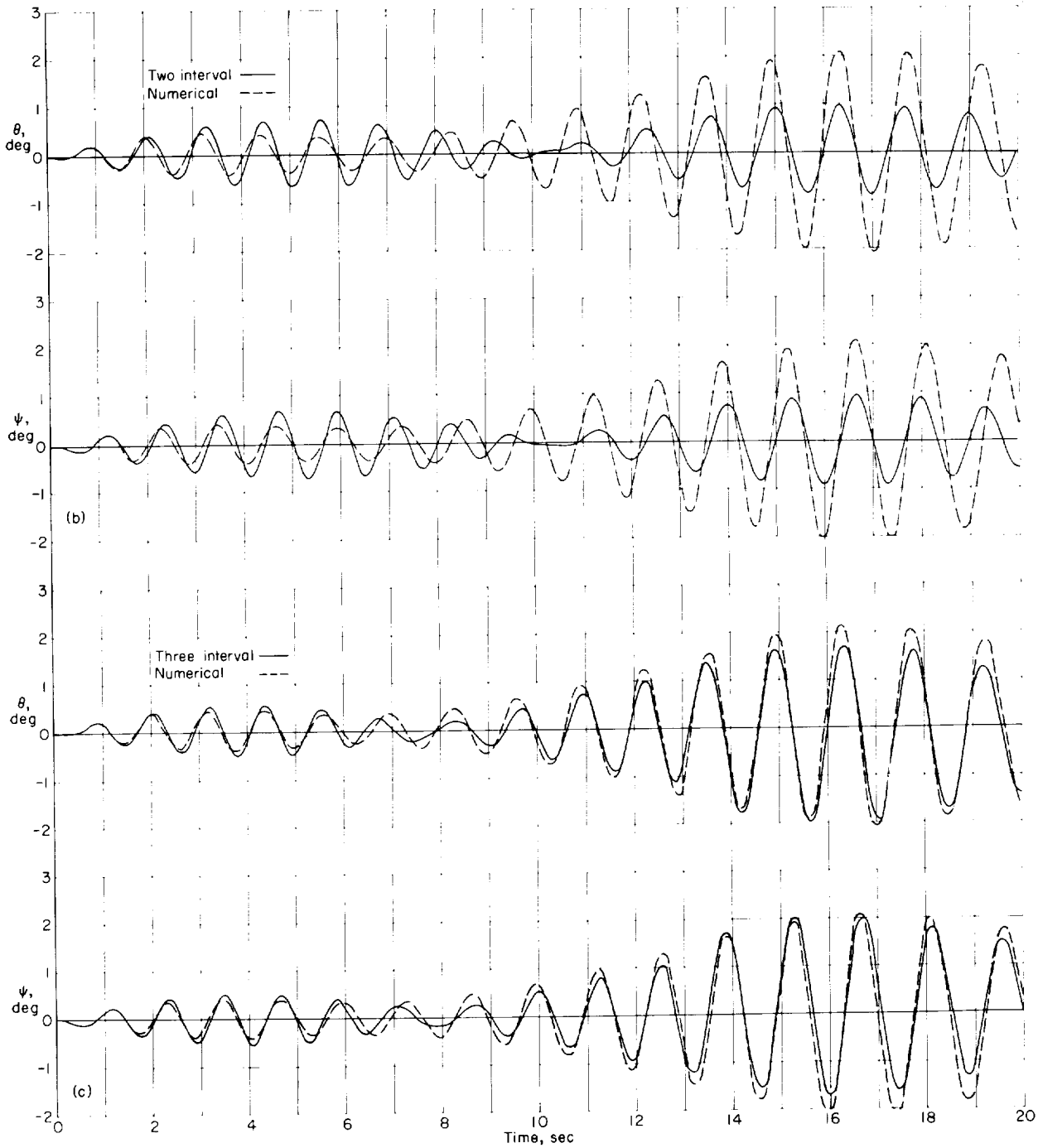

(b) Two-interval approximation.

(c) Three-interval approximation.

FIGURE 8.—Concluded.

CONCLUDING REMARKS

A method for approximating the vacuum motions of symmetrical rigid bodies with nonconstant spin rates and inertias has been developed. The analysis includes the effects of time varying thrust misalinements, mass unbalance, and jet damping. The method was derived for bodies having equal moments of inertia about their pitch and yaw axes and is based on body pitch and yaw attitudes being limited to "small angle" oscillations.

Results have been presented in the form of equations for space-referenced Euler angles, flight-path angles, and earth-referenced vehicle-trajectory coordinates. Equations for determining maximum wobble have been developed for certain input conditions. Also, equations for body-referenced attitude rates, angle of attack, and angle of sideslip are included for convenience.

The general solutions give insight into the individual effects of the variables and, in many cases, offer a quick means for obtaining approximate solutions. Although the method is somewhat lengthy for accurate hand computation in most cases, it is readily programed for automatic computer solutions.

The method has been shown to compare closely with numerical solutions of two sample problems. The sample problems also illustrated the relatively large effect of pitch and yaw jet damping on body motions.

LANGLEY RESEARCH CENTER,
NATIONAL AERONAUTICS AND SPACE ADMINISTRATION,
LANGLEY STATION, HAMPTON, VA., *April 24, 1961.*

APPENDIX A

EXACT SOLUTION WITH NONCONSTANT SPIN RATES

Combining equations (8), (11), and (13) results in the solution

$$\lambda=\lambda_o+e^{i\phi_o}\left\{A'(1+at)e^{i\frac{p_o}{a}\left(\frac{I_X}{I}\right)\log_e(1+at)}-A'-B'-C'-D'+[B'(1+at)^2+C'(1+at)^3+D'(1+at)^4]e^{i\frac{p_o}{a}\log_e(1+at)}\right\}$$

where

$$A'=\frac{\dot{\lambda}_o e^{-i\phi_o}}{a+ip_o\frac{I_X}{I}}-\frac{\frac{A}{a}-\frac{B}{a^2}+\frac{C}{a^3}}{\left[1+i\frac{p_o}{a}\left(1-\frac{I_X}{I}\right)\right]\left(a+ip_o\frac{I_X}{I}\right)}-\frac{\frac{B}{a^2}-\frac{2C}{a^3}}{2+i\left(\frac{p_o}{a}\right)\left(1-\frac{I_X}{I}\right)}-\frac{\frac{C}{a^3}}{3+i\left(\frac{p_o}{a}\right)\left(1-\frac{I_X}{I}\right)}$$

$$B'=\frac{\frac{A}{a}-\frac{B}{a^2}+\frac{C}{a^3}}{\left[1+i\left(\frac{p_o}{a}\right)\left(1-\frac{I_X}{I}\right)\right](2a+ip_o)}$$

$$C'=\frac{\frac{B}{a^2}-\frac{2C}{a^3}}{\left[2+i\left(\frac{p_o}{a}\right)\left(1-\frac{I_X}{I}\right)\right](3a+ip_o)}$$

$$D'=\frac{\frac{C}{a^3}}{\left[3+i\left(\frac{p_o}{a}\right)\left(1-\frac{I_X}{I}\right)\right](4a+ip_o)}$$

This result displays the spiral nature of the θ,ψ motion for nonconstant spin rates. Spin rates decreasing with time result in spiral motions of increasing magnitude and spin rates increasing with time act to reduce the magnitude of the θ,ψ motion.

APPENDIX B

SAMPLE PROBLEM INFORMATION

PROBLEM 1

Problem length, sec	20
Mass, slugs	$20-\frac{5t}{9}+\frac{5}{1,800}t^2$
Thrust, lb	$5,000-50t$
Pitch and yaw inertia, slug-ft^2	$25.6-0.53t$
Roll inertia, slug-ft	$3.93-0.0965t$
Roll input moment, ft-lb	0.572
Pitch input moment, ft-lb	$0.001(5,000-50t)(2+0.025t)$
Yaw input moment, ft-lb	$0.001(5,000-50t)(2+0.025t)$
Thrust arm, ft	$2+0.025t$
Initial flight-path velocity, ft/sec	5,000
Initial roll angle, radians	0
Initial pitch angle, radians	0.05
Initial yaw angle, radians	0.04
Initial roll rate, radians/sec	5
Initial pitch rate, radians/sec	0.015
Initial yaw rate, radians/sec	0.02
Initial flight-path angle in vertical plane, radians	0.02
Initial flight-path angle in horizontal plane, radians	0.01
Two-interval solution:	
Intervals	$0\leqq t\leqq 12,\ 12\leqq t\leqq 20$
Maximum change of p within the interval, percent	41
Maximum change of $p\frac{I_X}{I}$ within the interval, percent	33
Ten-interval solution:	
Intervals	2-sec intervals successively from 0 to 20 sec
Maximum change of p within the interval, percent	6
Maximum change of $p\frac{I_X}{I}$ within the interval, percent	4.6

PROBLEM 2

Problem length, sec	20
Pitch and yaw inertia, slug-ft^2	25
Roll inertia, slug-ft^2	$31.25-0.6973t$
Roll moment input, ft-lb	0
Pitch moment input, ft-lb	$-\frac{1}{2}$
Yaw moment input, ft-lb	0
Initial roll angle, radians	0
Initial pitch angle, radians	0
Initial yaw angle, radians	0
Initial roll rate, radians/sec	5
Initial pitch rate, radians/sec	0
Initial yaw rate, radians/sec	0
Initial flight-path angle, vertical plane	0
Initial flight-path angle, horizontal plane	0
One-interval solution:	
Maximum change of p within the interval, percent	0
Maximum change of $p\frac{I_X}{I}$ within the interval, percent	36
Two-interval solution:	
Intervals	$0\leqq t\leqq 12,\ 12\leqq t\leqq 20$
Maximum change of p within the interval, percent	0
Maximum change of $p\frac{I_X}{I}$ within the interval, percent	20
Three-interval solution:	
Intervals	$0\leqq t\leqq 6.7,\ 6.7\leqq t\leqq 13.3,\ 13.3\leqq t\leqq 20$
Maximum change of p within the interval, percent	0
Maximum change of $p\frac{I_X}{I}$ within the interval, percent	14

REFERENCES

1. Nicolaides, John D.: On the Free Flight Motion of Missiles Having Slight Configurational Asymmetries. Rep. No. 858, Ballistic Res. Labs., Aberdeen Proving Ground, June 1953.
2. Jarmolow, Kenneth: Dynamics of a Spinning Rocket With Varying Inertia and Applied Moment. Jour. Appl. Phys., vol. 28, no. 3, Mar. 1957, pp. 308–313.
3. Buglia, James J., Young, George R., Timmons, Jesse D., and Brinkworth, Helen S.: Analytical Method of Approximating the Motion of a Spinning Vehicle With Variable Mass and Inertia Properties Acted Upon by Several Disturbing Parameters. NASA TR R-110, 1961.
4. Perkins, Courtland D., and Hage, Robert E.: Airplane Performance Stability and Control. John Wiley & Sons, Inc., c. 1949, p. 380.
5. Davis, Leverett, Jr., Follin, James W., Jr., and Blitzer, Leon: Exterior Ballistics of Rockets. D. Van Nostrand Co., Inc., c. 1958, pp. 33–36.
6. Abzug, Malcolm J.: Applications of Matrix Operators to the Kinematics of Airplane Motion. Jour. Aero. Sci., vol. 23, no. 7, July 1956, pp. 679–684.

U.S. GOVERNMENT PRINTING OFFICE: 1963